Engineering Properties, Hydraulic Behaviour and Theoretical Modelling of Nuclear Waste Flows - 11098

S.R. Biggs[*], M. Fairweather[*], J. Young[*], J. Peakall[**], T. Hunter[*], J. Yao[*] and D. Harbottle[*]
[*]School of Process, Environmental and Materials Engineering, University of Leeds, Leeds LS2 9JT, UK
[**]School of Earth and Environment, University of Leeds, Leeds LS2 9JT, UK

ABSTRACT

A large amount of nuclear waste in the UK is stored in ponds as a solid-liquid slurry, and liquid flows containing suspensions of solid particles are encountered in the processing and disposal of this waste. The slurry systems encountered are complex and it is important to understand how particles interact and aggregate, their behaviour in terms of their settling and re-suspension characteristics, and the properties of deposited beds. A clearer understanding of these issues can allow the refinement of approaches to waste management, potentially leading to reduced uncertainties in radiological impact assessments, smaller waste volumes, lower costs and accelerated clean-up. This paper describes our research in three complementary areas that support the treatment of such waste, namely: the engineering properties of nuclear waste slurries; their hydraulic behaviour; and the theoretical modelling of such flows. Engineering properties have been studied by deconstructing the slurries' complex overall properties to singular particle-particle interactions, allowing the mechanisms involved in particle aggregation to be more readily understood, and the behaviour of flows in pipes has been examined to elucidate the influence they have on the particles in terms of their dispersion, deposition and re-suspension characteristics, and the influence the particles have on the flow. Lastly, computational fluid dynamic models are described, and their usefulness illustrated through application to duct flows, with their ability to predict detailed flow characteristics considered. Overall, the results described have enabled the characterisation of a range of particulate systems, with results pointing to a number of important factors that help to explain the observed variability in industrial slurry behaviour. Additionally, it has enhanced our understanding of, and ability to predict, flows of particles which in turn is of value in enabling the design of cost effective and efficient waste treatment processes.

INTRODUCTION

A large amount of existing nuclear waste in the UK is stored in ponds as a solid-liquid slurry, and liquid flows containing suspensions of solid particles are encountered in the treatment and disposal of this waste. The particulate systems encountered in these slurries are highly complicated, with their aggregation and flow behaviours being highly variable. Clearly, it is important to understand the way in which the solid particles interact and aggregate, and their subsequent behaviour in any flow in terms of their settling or non-settling characteristics, their propensity to form solid beds, the properties of those beds, and the re-suspension characteristics of particles from a bed. Once formed, solid beds are difficult to remove through the modification of process conditions alone, and prohibitively expensive to remove by manual intervention. A clearer understanding of these issues would allow the refinement of approaches to waste management, potentially leading to reduced uncertainties in radiological impact assessments, smaller waste volumes, lower costs, accelerated clean-up and reduced worker doses. This paper describes research underway at the University of Leeds in three complementary areas that support the treatment and disposal of such waste, namely: the engineering properties of waste slurries; their hydraulic behaviour; and the theoretical modelling of such flows.

To permit greater understanding of the engineering properties of slurries, deconstructing the complex overall slurry activity to singular particle-particle interactions allows the mechanisms involved in particle aggregation to be more readily understood, and hence to better predictions of their settling and flow in nuclear systems. Of particular importance to legacy waste is the role of salts in controlling the attraction of particles, and so in dictating the rheological properties of the system, as sludge's may contain a variety of specific ions and generally have high ionic conductivity. Work on the characterisation of particle-particle interactions using a number of complementary methods (e.g. atomic force microscopy, zeta-potential and shear/compressional yield stress measurement) under various salt and pH conditions is described, together with measurements of their influence on the characteristics of the aggregates and solid beds they form.

Knowledge of the behaviour of particle systems under flow conditions is the next stage of understanding required to support waste processing. Systematic studies of solid-liquid flows by experimental investigation are still limited for pipe flows, especially for fine particles, and research work is required to understand the effects physical parameters (e.g. particle shape, size distribution, solids concentration) on the properties of such flows, particularly in horizontal pipes where particles may settle out and form solid beds. Particles also modify the characteristics of any flow, thereby changing their ability to maintain particles in suspension. Work underway to examine pipe flows over a range of Reynolds numbers, and at varying levels of solids concentrations, is described, with measurements gathered using ultrasonic and laser-based techniques. Work to date has demonstrated the influence such flows have on the particles in terms of their dispersion, deposition and re-suspension characteristics, and the influence the particles have on the flow where the levels of turbulence can be significantly affected by their presence.

Lastly, mathematical models are of value in waste processing due to the diverse range of flows involved, e.g. in vessels, ponds, pipes and drains. To investigate experimentally all waste forms and potential flows of interest would be prohibitively expensive, whereas the use of models helps to focus experimental studies, identify data requirements, and reduce the need for process optimisation in full-scale trials. Validated models can also be used to predict waste transport and retrieval behaviour to enable cost effective process design and continued operation, to provide input to process selection, and to allow the prediction of operational boundaries. The paper describes work on the development and application of computational fluid dynamic techniques, coupled to particle tracking approaches, to meet these requirements. These methods can provide the detailed information on flow field characteristics and particle distribution required in the design process, and the usefulness of these techniques is illustrated through their application to duct flows, with their ability to predict detailed flow field characteristics, particle deposition and re-suspension considered.

The research described has enabled the characterisation of a range of particulate systems that may be encountered in legacy wastes, with results pointing to a number of important factors that help to explain the observed variability in industrial slurry behaviour. Additionally, it has enhanced our understanding of, and ability to predict, flows of particles which is of value in enabling the design of cost effective and efficient waste treatment processes.

ENGINEERING PROPERTIES OF NUCLEAR WASTE SLURRIES

Background

This section presents an overview of the techniques available to study the engineering properties of particles of relevance to nuclear waste slurries. Key results are described in relation to the characterization of particle properties obtained using a model titania simulant (oxide particles are commonly found in legacy nuclear waste ponds). Each technique is first described, followed by some results and a brief analysis. A discussion section follows, linking these complimentary techniques and highlighting their potential significance to the important industrial problem.

Facilities and Experimental Methodology

The materials used in the experiments and the preparation of suspensions for analysis is first described. A commercially available sample, ANX titania, was used for the work considered below. Chemical analysis showed that this material included a mixture of titanium dioxide (55-70)±0.1 wt% and titanium hydroxide (40-45)±0.1 wt%. All measurements and calibrations were performed at 22±0.1°C. The suspensions were prepared at 4.0±0.1 wt% solids for zeta potential measurements, and 47.0±0.1 wt% solids (titania) for rheological measurements. Monovalent chloride and nitrate salts of concentration 0.001-1.0 M were used in the titania suspensions. In addition, divalent sulphate and nitrate salts such as Na_2SO_4 and $Mg(NO_3)_2$ were also used to investigate the effects of alkali-earth metals for zeta potential measurements. The base and acid were chosen such that the same counter ions as the salt investigated were used so as not to introduce other ions into the system. All water used was distilled before ultra purification with activated carbon and ion-exchange resins (Milli-Q: conductivity $< 1 \times 10^{-6}$ Ω^{-1} cm^{-1} at 20°C), and was free of any organic and other impurities. Samples were allowed to stand or were rolled on a moving table for 24 hrs prior to any experiment. This allowed surface adsorption and complete homogeneous mixing throughout the sample. For the rheological measurements samples were allowed to age for 48 hrs on a roller prior to measurements.

Electroacoustic analysis was used to determine the electrokinetic properties (or zeta potential) as a function of the pH of the liquid phase. The zeta potential is used to correlate particle surface charge (which cannot be measured

directly) which is calculated from the dynamic mobility of particles under an applied voltage considering material properties (such as density of the solid and liquid viscosity), assuming the thin double-layer model [1-3]. Any particle with an anionic surface charge obtains a tightly bound cationic or counter ionic layer called the Stern layer around its surface. Moving further from the surface, a layer with mainly counter-ions and some co-ions is obtained. The electrical double layer (EDL) is therefore made up of two layers; an inner region (Stern layer) where the ions are strongly bound and an outer (diffuse) region where they are less firmly associated. The zeta potential is a measure of the charge close to the layer of bound ions and so is not a direct measurement of the surface potential. It is, however, used as a guide for determining the stability in a solid-liquid system and as a way of understanding which ions have the most significant effect.

In a typical experiment, each sample was transferred to the ZetaProbe® and stirred at a speed of 260 rpm for 10 minutes before the mobility was determined as a function of pH. The zeta probe measures a dynamic mobility spectrum and then calculates the zeta potential using the O'Brien model [1-4]. The electrolyte ions produce an electrokinetic sonic amplitude (ESA) signal of their own, which can be a significant portion of the total ESA signal at salt concentrations above approximately 0.01-0.1 M. In all cases, the background electrolyte signal was measured and subtracted from the total signal so that the zeta potential error obtained was less than 5%. Each experiment was repeated at least four times and the results showed repeatability of the data. The titania 'simulant model' solid at 4 wt% was adjusted with appropriate base or acid of 0.1 M concentration to titrate the suspension. After pH adjustment, the suspension was allowed to equilibrate for 5 mins before the zeta potential measurement was performed. The suspension pH was monitored automatically using a pH electrode coupled with the zeta probe. Suspensions of titania material were prepared in a background electrolyte of analytical grade salts.

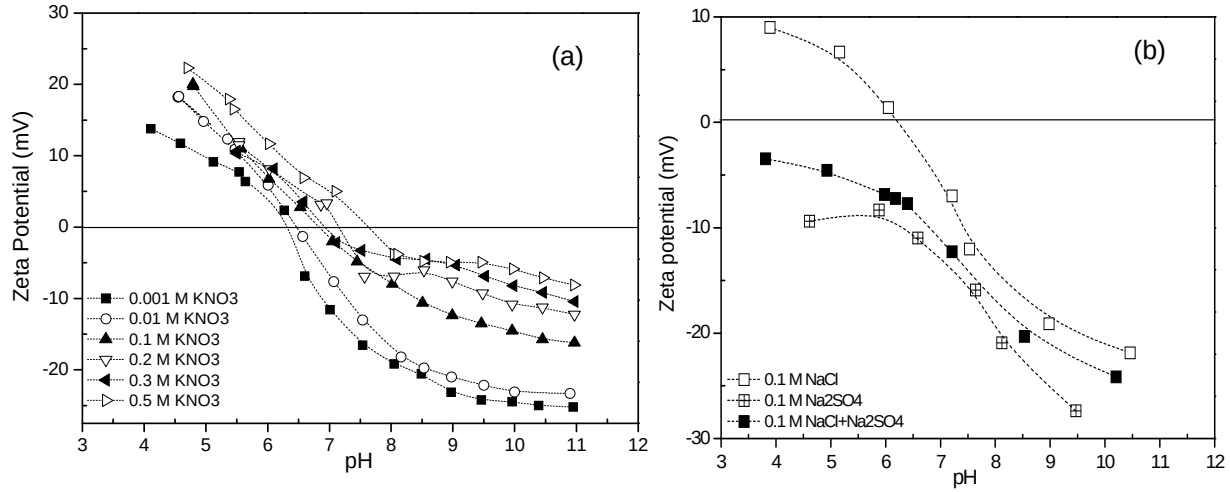

Fig. 1. Zeta potentials of titania as a function of pH and (a) potassium nitrate (KNO_3) salt concentration, and (b) salt type (single monovalent -□-, single divalent -⊞- and mixed -■-) for 0.1 M electrolytes.

It should be noted that 4 wt% particle dispersions were selected on the basis that they gave high signal to noise ratios, but in addition were low enough that the particle-particle interactions did not significantly affect the signal. Background electrolyte corrections were performed for all concentration series, though at the lowest concentration (0.001 M) the corrected and uncorrected results showed no significant difference. In contrast, at 0.01 M there was an evident difference of about 3 mV in the uncorrected zeta potential results. Some sample results illustrating the influence of electrolyte concentration are given in Fig. 1(a). Approximately S-shaped curves are observed at the lowest electrolyte concentration in this figure. These data curves gradually become flatter as the electrolyte concentration increases. The pH at which the electrokinetic isoelectric point, where the zeta potential equals 0 mV, occurs is within the average range 6.0-7.8. Once the effect of electrolyte concentration was quantified for all salts used, as shown in Fig. 1(a), zeta potential measurements of particle dispersions in different electrolytes were compared. A constant salt concentration of 0.1M was used, as it was assumed these concentrations approach conditions in legacy waste slurries. Given in Fig. 1(b) is a series of results showing that particle zeta potential (and hence surface charge) changes significantly with solution pH in different electrolyte combinations.

Atomic force measurements (AFM) of interaction forces were obtained with the NanoScope IV AFM from Digital Instruments. Here, a flat titania substrate (mounted on a piezoelectric tube) is driven in a controlled manner towards and away from a titania colloidal probe mounted on an AFM tip. A laser monitors the movement of the colloidal probe tip, and hence the attraction or repulsion of the titania under different conditions. Force interaction plots for the titania probes at pH 9 with different electrolytes at high concentration (0.1 M) and low concentration (0.01 M) were obtained. These results show that at high salt, all relationships gave a small attraction, while at low concentration, there was a small attraction for the salt mixture, but a small repulsion for each individual electrolyte.

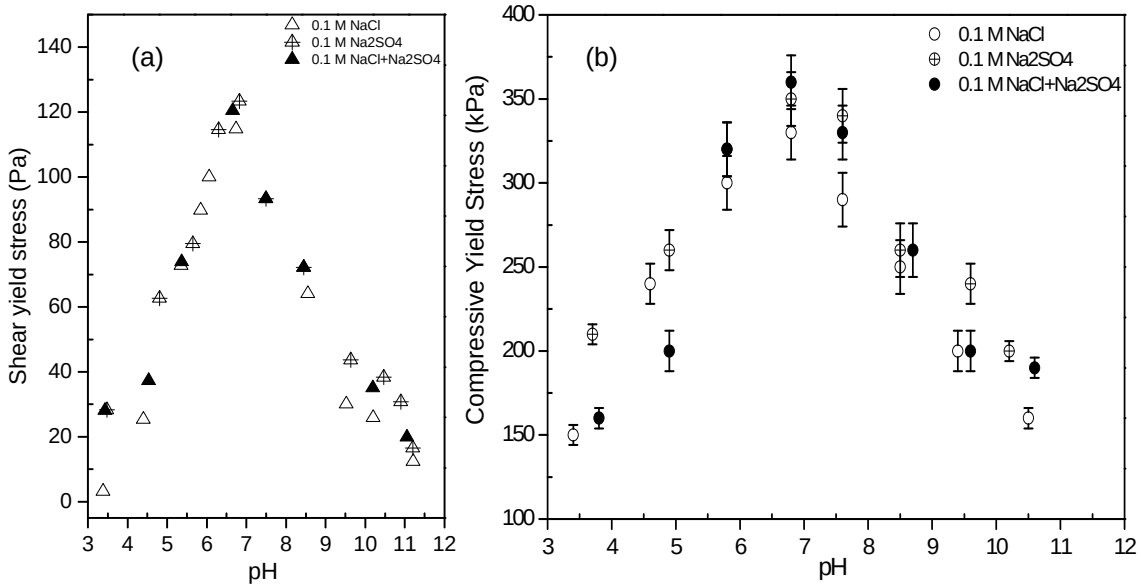

Fig. 2. (a) Shear yield stress of titania as a function of pH and salt type (single monovalent -Δ-, single divalent -⧋- and mixed -▲-) for 0.1 M electrolytes, and (b) compressive yield stress of titania as a function of pH and salt type (single monovalent -○-, single divalent -⊕- and mixed -●-) for 0.1 M electrolytes.

Shear yield stress measurements were performed using the vane technique of Nguyen and Boger [5]. The experimental apparatus consists of a small four-bladed vane attached to the spring-driving motor of a Brookfield viscometer. The spindle is driven by a motor through a calibrated spring; deflection of the spring is indicated by a digital display. The vane is immersed in the suspension, and torque and viscosity response are measured as a function of time as the tool is rotated at a slow constant rate, and these data are then related to the shear yield stress [5, 6]. A key benefit of the vane spindle is that it imparts a minimal disruption to the sample during immersion. Fig. 2(a) demonstrates how the yield stress depends directly on the pH, and hence the zeta potential, with a maximum at pH values close to the isoelectric point or, in other words, where the particles surface charge is minimized.

Compressive yield stress measurements were obtained using a piston/compression rig. This is a bespoke rig, specifically designed to allow testing of nuclear waste slurry simulants, and can measure yield stresses up to 450 kPa. Here, the pressure is stepped up in each filtration run to determine the compressive yield stress $P(\phi)$. The compressive yield tests are conducted at the lowest pressure desired until equilibrium or an end point is reached as $\phi \rightarrow \phi_\infty$. The compressor rig employs a pneumatic cylinder to apply pressure to a sample contained in a compression cell, forcing liquid out through a filter membrane at the base of the cylinder which is supported by a permeable sintered metal disk. The pressure of filtration is monitored using a pressure transducer mounted flush in the piston face. The rate of filtration is monitored through the rate of movement of the piston, with the movement of the piston tracked using a linear encoder with a spatial resolution of 10 μm. After the piston has settled to equilibrium from the initial pressure, the pressure is stepped up to a higher level and filtration is permitted to proceed again to equilibrium. The pressure control system allows pressures ranging from 1 up to around 400 kPa to be tested, depending on the sample being tested and the degree of friction inside the compression cell. The pressure is incremented once more and the procedure is repeated. The pressure at every step is the compressive yield stress for the solid volume fraction at equilibrium ϕ_∞. Fig. 2(b) shows the compressive yield stress results under the same conditions as the shear yield stress. As is clearly observed, qualitatively the same relationship holds as for the shear

yield stress, with values increasing near the isoelectric point, where the particles have their lowest charge (and so are least mutually repulsive). Because of the nature of this test method, there is a higher error value of approximately ±15, especially near the isoelectric point (least unstable region).

Results and Discussion

The zeta potential measurements in Figs. 1(a) and (b) highlight some key changes to particle-particle interactions with pH, which significantly influences slurry rheology. At high pH, all dispersion-electrolyte mixtures show large negative values, inferring the particles have high negative charge and are repulsive. As pH is decreased, the magnitude of the surface charge is reduced, and the zeta potential reaches a minimum in magnitude around pH 6-7. The monovalent electrolyte dispersions (KNO_3 in Fig. 1(a) and NaCl in Fig. 1(b)) actually cross a point of zero charge at approximately pH 6.5-7.5 before the charge inverts to a positive value, whereas the divalent salt (Na_2SO_4) and mixed salt dispersion charges seem to level off around this pH (Fig. 1(b)). It is interesting that both the electrolyte dispersions containing divalent salts give a similar relative change in behaviour, indicating that there is specific ion adsorption occurring with the divalent salt mixtures onto the particle surfaces, thus changing the zeta potential profile expected. The similarity in behaviour between the divalent and mixed electrolyte dispersions also indicates that the divalent salt is dominating the interactions with the particle surfaces. It is also observed in Fig. 1(a) that for the single KNO_3 salt at varying concentrations, the isoelectric point shifts as a function of electrolyte concentration; an effect that is indicative of a specific adsorption of ions at the solid-liquid interface. Specific chemical adsorption implies some direct bonding between surface atoms and partially or fully dehydrated solution ions in the compact EDL regions. Specific physical adsorption generally occurs due to the attractive van der Waals interactions between the surface and ions from the bulk solution.

Although not shown, the AFM force curves illustrated further behaviour that is critical in defining slurry activity. At high salt conditions all dispersions showed an attraction between the titania probe and substrate. This is despite the fact that these tests were conducted at pH 9, and thus (from the data in Fig. 1(b)) the particles are all highly negatively charged, and so should be mutually repulsive. The reason for this apparent contradiction is the interaction of the salt in reducing the charge double layer of the particles [7]. In effect, the salt reduces the extent of solution counter-ion layer around the particles, reducing the interaction distance between neighbouring particles. The charge layer is reduced to such an extent that attractive Van der Waals forces [7] begin to dominate and the particles attract. The significance of these AFM results, in terms of legacy waste behaviour, is that, despite often being in very alkaline environments, if salt conditions approach those used in these tests, the oxide particles will likely be forced into a state of coagulation and aggregation. Any aggregation will critically affect their rheological and settling behaviour. It is an interesting aside that at low salt concentrations each individual salt also showed purely repulsive behaviour, while the mixed salt still showed an attraction. These contrasting results point to further complex interactions of the salts at the particle surfaces. However, low salt conditions are not as relevant to legacy wastes.

Both sets of yield stress data highlight the importance of particle surface charge in determining rheological behaviour. The yield stresses reach an approximate maximum at a pH relating to the point of minimum surface charge (isoelectric point). Because of the likely coagulated or aggregated nature of the particles, due to the high salt, they are most probably arranged into open, interconnected flocs [8, 9]. The strength of these flocculated networks is clearly dependent on the surface charge of the particles, and is heightened under conditions where the particles are least repulsive to one another. Both compression and shear yield tests show the same behaviour, but the maximum yield stresses in the compressional tests were about 2-3 orders of magnitude higher than the shear values (Figs. 2(a) and (b)). This is probably due to the increase in pressure of liquid being pushed through the bed under compression. Also, this result shows that the forces required to press the particulate beds (as in the case of dewatering) are far greater than those required to shear the bed apart. This has important consequences for the processing of the settled legacy waste beds, implying redispersion mechanisms utilising a shearing action would be more energy effective.

All electrolyte dispersions gave the same yield stress trends, but do show some interesting interactions between the monovalent and divalent salts. Similar to the zeta potential data, the compressional yield stress data (Fig. 2(b)) and to a lesser extent the shear yield data (Fig. 2(a)) suggest that the mixed monovalent and divalent salt behaviour is more closely aligned to the single divalent salt behaviour (at least around the peak stress values). Again, this indicates that the divalent salt is dominating the interactions with particle surfaces, and the influence of the monovalent salt is reduced. In terms of potential industrial significance, this suggests that the potentially complicated systems found in legacy wastes, where various salts may be in competition with one another, can be

simplified. In essence, if the high valance salts can be identified, the influence of any other low valence salts present may be largely ignored, allowing greater focus on the most significant electrolyte contributions to particle-particle interactions and slurry rheology.

HYDRAULIC BEHAVIOUR OF NUCLEAR WASTE SLURRIES

Background

The transport of slurries in pipes is widely used across many sectors, and the flow properties of such systems have been extensively studied, although generally not to the level required to generate fundamental understanding of particle transport. Traditionally, the accepted view within the nuclear industry is that dispersions of solids should be pumped as relatively dilute slurries (i.e. solid volume fraction < 5%). This is considered to be the safest option since it minimises or avoids any potential for pipe restrictions and/or blockages. The industry has comparatively low volumes of sludge compared to those found in other industries, however, they are substantially more problematic due to the inability to take samples and thereby obtain meaningful characterisation data. The pipeline transport of highly concentrated tailings is, however, standard practice in the mineral and mining industries. Research into tailings, which contain a high percentage of surface-active, sub-micron particles, has lead to the optimisation of mixing and pumping processes. The use of rheological modifiers to avoid plug formation during transport, to improve hydraulic pumping gradients and to avoid sediment compaction during process shutdown has been an area of active interest for the last 20 years. The information collected whilst studying such operations is applicable to the nuclear industry, where waste management projects are encountering issues with dense sediment conveying.

The material to be transferred from existing nuclear facilities can be categorised into three groups: fluid (very few particulates); slurry (low to intermediate particle concentrations with Newtonian/non-Newtonian behaviour); and pastes (high solids concentrations with non-Newtonian behaviour). The last two categories contain enough fine particles that the slurry/paste chemistry can influence the conveying nature of the material. The rheological behaviour of these wastes can therefore be influenced by controlling particle-particle interaction forces, thereby potentially permitting the transport of solids at a high volume fraction.

The present work considers two areas of relevance to the transportation of fine colloidal particles that are of interest to the processing of nuclear waste. The first concerns the minimum transport velocity for the transfer of particulates in a pipe flow. Colloidal spheres were used so that the effect of particle clustering could be investigated, with the degree of aggregation controlled by electrolyte concentration. The second concerns the influence of two colloidal suspensions on turbulence levels within a pipe flow. This study is of direct practical relevance since the energy input required to maintain particles in suspension can be lowered in the presence of aggregates, with any energy "deficit" overcome by the turbulence enhancement caused by such particles. The latter issue, in particular, has been of great interest in recent years, where it has been shown that the addition of particles to a fluid can act to enhance or dampen the fluid turbulence. Gore and Crowe [10] considered turbulence modulation by examining a number of data sets, and by comparing the turbulence intensity as a function of particle diameter (d_p) and the characteristic length of the most energetic eddies (l_e) they concluded that there is a critical length scale (d_p/l_e) where a transition from turbulence attenuation to augmentation is observed. This length scale is found to be ≈ 0.1, such that at values > 0.1 turbulence augmentation occurs due to secondary flows (vortex shedding) associated with the particles. Turbulence attenuation ($d_p/l_e < 0.1$) during the transportation of fine particles occurs as a result of work done by the turbulent eddies.

Particle clusters (aggregates) are formed when solids become surface active. For example, ionisation when a solid is dispersed in an aqueous electrolyte solution can lead to the formation of aggregates. In an aqueous electrolyte environment very fine particles (colloids) exhibit extremely low inertial forces; as a result the surface charge plays a significant role in their interaction, partially governing the size and shape of the aggregate. Open porous aggregates are formed under conditions that are commonly referred to as diffusion-limited, cluster-cluster aggregation, DLCA [11]. DLCA occurs when the dispersive component for particle stability is negligible, leading to a situation where all collisions result in a sticking event producing large open porous clusters which are unlikely to undergo rearrangement to produce more compact clusters. With a small potential barrier to aggregation the probability of a sticking event when the particles come into close proximity is reduced. The aggregation kinetics are suitably described by the reaction-limited, cluster-cluster aggregation, RLCA, model [11], where the particles have an opportunity to diffuse into the core of the aggregate before they become attached. This mechanism, which is limited by the reaction of the particle to the cluster particles, produces smaller more compact aggregate structures.

The interaction potential between colloidal particles is described by the DLVO [7, 12] theory, and is given as the sum of the attractive van der Waals potential and the electrical double layer repulsive potential. When two like surfaces approach, there is a like-like charge repulsion effect which prevents the surfaces from intimate contact. However, the surface charge can be effectively "screened" by increasing the ionic concentration of the solution, which allows the surfaces to approach to within a shorter separation distance before they begin to repel. As the ionic concentration of the suspension increases, the thermal energy barrier preventing interaction decreases, and a condition can be met where the kinetic energy of the particles is sufficient to drive the surfaces into contact. Upon contact, the surfaces are likely to "stick" forming aggregates which can be several orders of magnitude greater in size with respect to the primary particle.

With improvements in attrition technologies and the advancement of "bottom-up" engineering applications, colloidal particles and their handling is becoming increasingly more important in the process industries. In the studies described below, the importance of solution chemistry when transporting fine particulate solids is highlighted in applications of relevance to nuclear waste processing.

Facilities and Experimental Methodology

The work described below was conducted in the Sorby Environmental Fluid Dynamics Laboratory (SEFDL) at the University of Leeds. This laboratory supports research into the fluid dynamics and sedimentary processes of both natural environments and industrial processes, and is one of the leading fluid dynamics laboratories in Europe, and amongst the best equipped laboratories of its type globally. The SEFDL encompasses a number of major flumes, including three re-circulating open-channel flumes, three gravity current tanks, a large stream table, a flow loop and a facility for the study of jet impingement. The laboratory also hosts an array of flow measurement techniques, including a range of techniques for velocity and particle concentration measurements.

A horizontal pipe flow loop was used in the experiments described below, consisting of an open, re-circulating 26 mm N.B. pipe loop with PVC-U and glass piping. The loop contains a 5.5 m test section of clear pipe which is secured to a horizontally leveled bench, with an outbound and inbound length of 2.3 m and 2.5 m respectively, and with the test section preceded by a disturbance free approach length which allowed the development of fully developed flow. A 620 SN/RE peristaltic pump with a 17 mm diameter Marprene TM tubing element provides flow rates up to Re=11,000, with small pulsations damped by a 2 m coil of un-reinforced PVC hose. A magnetic inductive flow meter with a 6 mm measurement bore capable of measuring flow rates up to Re=15,000 is installed on the vertical section of piping.

An ultrasonic Doppler velocity profiling (UDVP) sensor positioned at 45^{o} to the flow axis in the fully developed section of the flow loop was used to collect velocity profiles within the pipe over a 30 s period. Velocity profiles were collected at several flow rates, with each measurement collected after 1 min of steady-state flow. At an equivalent flow velocity the sediment-free and particle-laden velocity profiles were compared to identify the region of velocities at the onset of particle deposition. The fluid turbulence was quantified in terms of root mean square values of the fluctuating streamwise velocity component of the flow, calculated from measurements of the instantaneous velocity and the derived mean streamwise velocity. The onset, or transition, velocity for sediment bed erosion was determined from flow images collected using a 15 Hz NewWave Solo particle image velocimetry (PIV) II-15, 30mJ, 532nm, Nd YAG laser coupled with a digital camera. Suspensions of known concentration were circulated in the pipe loop at a flow velocity greater than the heterogeneous transitional velocity. After 10 mins the flow was stopped and the test section isolated, with the remaining suspension drained from the pipe loop. Once a fully consolidated sediment bed had formed, the drained suspension was agitated and pumped back into the pipe loop. At a given volumetric flow rate the sediment bed height was measured over the first 30 s, and the average flow velocity determined using an equivalent pipe diameter. The transition velocity as a function of the consolidated bed height (solids loading) was then extrapolated to zero bed height to determine the minimum transport velocity.

An ultra high purity (> 99.5% SiO_2), near mono-disperse, silica sample was employed in the experiments. This sample had a density of 2260 kg m^{-3}, determined using a Micromeritics AccuPyc 1330 pycnometer, and a mean particle diameter of 0.79 μm, measured using a centrifugal sedimentation particle size analyser. All chemicals and other reagents were of analytical grade. The experimental programme used both low and high solids concentrations. Two slurries, one at 1M KNO_3 and the other at 10^{-4}M KNO_3, were prepared in 40 litre batches to a solids concentration of approximately 6% by volume for the low concentration, and 12% by volume for the high

concentration. The in-situ solids concentration for each experiment was determined through oven drying a one litre sample of slurry collected from the pipe loop discharge. All slurries were prepared 24 hrs in advance of the pipe loop study, with the suspension pH monitored and adjusted to pH 6 using 5M complementary analytical grade acid and base. A paddle mixer was used to periodically agitate and disperse the solids in suspension prior to the slurry being transferred to the feed vessel. Colloidal silica spheres prepared in 10^{-4}M and 1M KNO_3 electrolytes at pH 6 were used since these two conditions give significantly different zeta potentials and, therefore, different particle/cluster structures. When the 0.79 μm silica spheres were dispersed in the two electrolytes, therefore, the particles remain dispersed when prepared in 10^{-4}M KNO_3, while in 1M KNO_3 they formed chain and spherical like structures, a result of a strong attractive interaction force between neighbouring particles.

Results and Discussion

In terms of the minimum transport velocity, velocity profiles for particle-laden and sediment-free flows were compared at equivalent bulk flow velocities, and UDVP was used to identify those conditions when the two profiles diverged and the particle-laden mean velocities were exceeded by those of the sediment-free flow. This indicates an increase in the fluid drag which is related to the stratification and deposition of particles. This work established that at a bulk velocity of 0.19 ms^{-1} the differential velocity can be considered negligible. With a reduction in this velocity to 0.15 ms^{-1} small deviations in mean velocities were observed at the pipe wall, suggesting particle stratification and deposition. Further reducing the velocity to 0.11 and 0.07 ms^{-1} led to greater differential velocities at the wall, a result of increasing stratification of the suspension when the mean velocity is below the minimum transport velocity. The results obtained suggest that the minimum transport velocity for the 10^{-4}M KNO_3 and 1M KNO_3 suspensions is in the region of 0.19 and 0.15 ms^{-1}, respectively. The minimum transport velocity was also determined using PIV by measuring the sediment bed erosion rate as a function of the bulk flow velocity. Above a critical streamwise velocity the sediment bed erosion rate changed from negative erosion (deposition) to positive erosion (bed height decrease), with the erosion rate increasing with the bulk velocity. The transition velocity, taken as the zero erosion rate, as a function of the sediment bed height could then be plotted, as shown in Fig. 3(a).

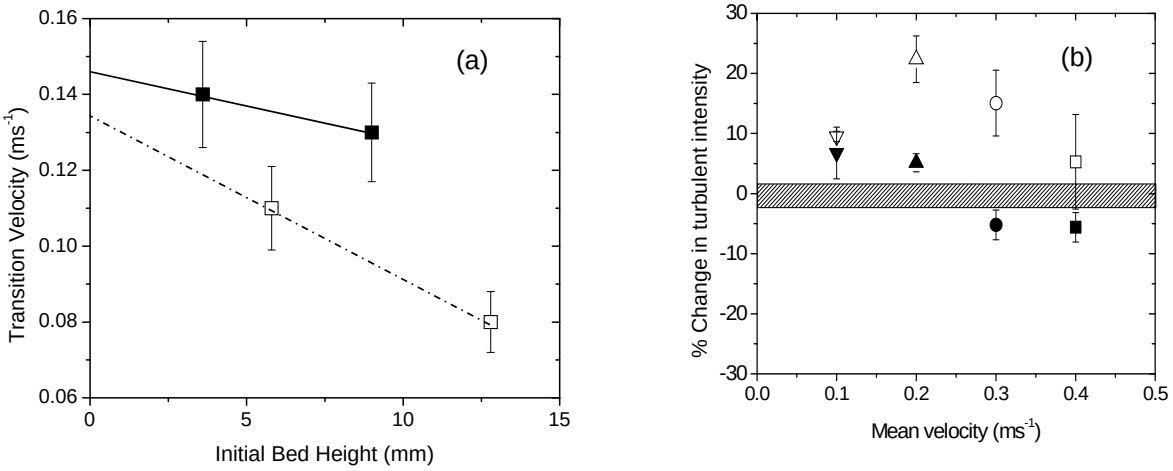

Fig. 3. (a) Slurry transition velocities as a function of sediment bed height (open square – 1M KNO_3, closed square – 10^{-4}M KNO_3), and (b) percentage change in centre-line turbulence intensity relative to water (open symbols – 1M KNO_3 at 5.7% vol., closed symbols – 10^{-4}M KNO_3 at 5.5% vol., shaded region – water).

The data of Fig. 3(a) demonstrate that, independent of electrolyte concentration, the transition velocity decreases as the initial sediment bed height (solids loading) increases. For a given sediment structure, which is dependent on the particle-particle interaction strength and the number of particle-particle contacts, the force required to initiate sediment bed erosion can be calculated from the critical bed shear stress. For the concentrations investigated the values of this parameter for a 10^{-4}M KNO_3 sediment (weakly attractive) and a 1M KNO_3 sediment (strongly attractive) are 0.05 and 0.26 Pa, respectively. With the critical bed shear stress dependent on the electrolyte type, but independent of solids loading, it is reasonable to extrapolate the data to zero bed height to determine the minimum

transport velocity for the dispersed and aggregated fine particulate suspensions. This gives a minimum transport velocity for a 10^{-4} M KNO_3 suspension ≈ 0.15 ms^{-1}, and for a 1M KNO_3 suspension in which the particles form clusters a value ≈ 0.13 ms^{-1}. These velocities are within reasonable agreement with the data obtained using UDVP. The results of Fig. 3(a) also demonstrate that the measured transition velocities for 1M KNO_3 (aggregated) suspensions are lower than those for 10^{-4}M KNO_3 (dispersed) suspensions. This finding is counter-intuitive when considering the difference in particle size and sedimentation rates, i.e. the measured sedimentation rate of the aggregated suspension is approximately 25 times the rate of the dispersed suspension. These differences may be related to the turbulence properties of the suspension, as discussed further below. In particular, centre-line variations in the streamwise turbulence intensity for an aggregated, dispersed and sediment-free flow show a clearly enhancement for the aggregated suspension. This enhancement in turbulence provides support to the minimum transport velocity results, since fluid turbulence provides the driving energy to maintain particles in suspension.

Turbulence intensities (i.e. streamwise fluctuating velocity/depth-averaged mean velocity) of the aggregated and dispersed suspensions were measured at equivalent solids concentrations in pipe flows. A clear enhancement in the near-wall turbulence was observed when the suspension was aggregated which extended beyond the buffer layer into the mainstream region of the flow. In the buffer layer, the turbulence intensity will be a function of the fluid-wall, particle-fluid, particle-wall and particle-particle interactions. However, particle relaxation times are smaller than the characteristic time of the energy containing eddies, such that the particles should follow the flow, neither dampening nor enhancing the intensity, and particle Reynolds numbers for the primary particle and aggregate are sufficiently low that neither should influence the fluid-wall or particle-fluid interactions. At the high solids concentrations used, a cumulative effect may result where small interferences between the fluid and particle, which are negligible at low concentrations, become significant and affect the turbulence intensity. For example, particle collisions with the pipe wall and with each other generate small scale fluctuations which in dilute flows will be negligible, while in concentrated flows the effect may become measurable. Small differences in near-wall velocity gradients may also be responsible, since an increase in such gradients provides a more favourable environment for the production of turbulence, with the aggregated suspension having the largest gradient of the cases considered.

The centre-line variations in turbulence intensity observed are summarised in Fig. 3(b) in terms of the percentage change in intensity as compared to a sediment-free flow. The intensities of a dispersed suspension do not appear to deviate significantly from those of the sediment-free flow, with the transition from turbulence augmentation to attenuation with increasing mean flow velocity within experimental error. However, the data do suggest that the centre-line intensities are enhanced in the presence of an aggregated suspension. At the wall, enhanced turbulence can be accounted for by particle-wall interactions, whilst at the centre-line the intensity can only be influenced by particle-fluid and particle-particle interactions. Typically, centre-line intensities are influenced by vortex shedding from wakes behind particles [10, 13] and changes in the fluid viscosity [14]. In this study, interpretation of the experimental data and critical analysis of the observed behaviour is difficult since no comparable data sets are available. Commonly, however, when the particle length scales are significantly smaller than the Kolmogorov scale, relatively small changes in turbulence intensities are frequently associated with a change in the suspension viscosity.

Possible reasons for the observed enhancement in centre-line intensities may be related to variations in micro-hydrodynamic disturbances at solid-liquid interfaces, which can result from; inter floc flow fields in an open porous structure [15], changes in the hydrodynamic drag or changes in the angular rotation rates of the particles. Because of the concentrated nature of the suspensions examined, information on particle rotation and slip velocities could not be collected. A clear difference in the particle size and shape in an aggregated suspension was, however, noted, which may lead to the development of complex flow fields and enhanced fluid disturbances. Further work examined the root mean square values of the streamwise fluctuating component of the single phase fluid, dispersed and aggregated suspensions, and an additional dispersed suspension containing silica spheres with a mean diameter of 27μm. These results illustrated the changes in fluctuating values as the flow progressively developed into fully developed turbulence, showing a sharp peak in the flow fluctuations around the transition region, attributable to intermittent turbulence in the form of turbulence puffs [16]. Above a critical Reynolds number (Re ≈ 5,500) the fluctuating streamwise component for an aggregated suspension exceeded those measured in a sediment-free and dispersed suspension flow, with the increase corresponding to the enhancement in turbulence intensity. This enhancement in values for the aggregate correlated with the enhancement in values for the dispersed suspension containing 27μm particles. The larger silica spheres which interact more with the fluid, and cause vortex shedding, appeared to modulate the turbulence to the same extent as the smaller aggregates. As the Reynolds number exceeded Re ≈ 8,000 the profile of the aggregated suspension began to converge with the dispersed suspension and sediment-free profiles.

Such behaviour is likely to be caused by the flow reaching a critical fluid shear stress beyond which the aggregates undergo gradual break-up. Further validation for this contention was provided by rheometer measurements which demonstrated that the aggregated suspension gradually decreased in viscosity and converged to that of the dispersed suspension at a shear rate of $\approx 100\ s^{-1}$, which corresponds well with the pipeline pseudo-shear rate.

THEORETICAL MODELLING OF NUCLEAR WASTE FLOWS

Background

As previously noted, mathematical models are of value in waste management since the processing of waste involves a diverse range of flows which cannot all be investigated experimentally. Validated models can also be used to predict slurry transport and retrieval behaviour to enable cost effective process design, to provide input to process selection, and to allow the prediction of operational boundaries. The particle-laden flows of interest can be broadly classified into three categories [17] on the basis of inter-particle collisions: collision-free (dilute) flows, collision-dominated (medium concentration) flows, and contact-dominated (dense) flows. Only the first type of flow is considered below. In terms of waste processing, procedures capable of handling dilute flows are required, as are ones that can accommodate medium flows (up to 20-30% solids by volume). For the latter, it is necessary to be able to predict the ways in which particle interactions occur, through modelling of particle interaction energies, and how particle agglomerates are formed. Providing a modelling capability for all these flows is a difficult task, and remains an area of active research, although the provision of such models is required if those phenomena of relevance to waste processing, such as particle deposition and re-suspension, are to be predicted.

Comprehensive reviews of the types of mathematical model available for predicting particle-laden flows are available [17-21]. Included are Lagrangian descriptions of particles, coupled with direct numerical simulation (DNS), large eddy simulation (LES) or Reynolds-averaged Navier-Stokes (RANS) solutions for the carrier phase [20]. Alternatively, Eulerian descriptions of both phases are possible through RANS and transported probability density function methods [20]. In Lagrangian-based simulation, particle motion occurs due to forces generated by the moving fluid, e.g. the fluid drag force. The particles can also be acted upon by other forces, e.g. gravity, electrostatic, etc., and all these forces, together with Newton's second law, govern their trajectory in the flow. The carrier phase also experiences reaction forces from the particles, and flow field modifications due to their presence couple the Lagrangian particle and Eulerian fluid phase simulations. Analysis of particle motion in a Lagrangian framework is accurate, applicable to dilute and medium concentration flow, can tackle particle collisions and the forces acting on a particle, and is easy to implement computationally. Lagrangian particle tracking is therefore numerically attractive and applicable to the flows of interest, and is used as the basis of the work described.

DNS of the turbulent flow equations, coupled to Lagrangian simulation of the particle phase, would describe completely a two-phase flow. However, the use of DNS is prohibitively expensive for the high Reynolds number flows of interest. As an alternative, LES can be employed. In LES, the governing equations of fluid flow are filtered to separate large- and small-scale turbulent motions, with the large-scale solved for directly, and the small scales modelled through a sub-grid scale model. The trajectories of particles are then calculated on the basis of the LES generated flow field. In RANS, the equations of fluid flow are time-averaged. This results in a loss of information, meaning that unknown terms in the resulting equations, the Reynolds stresses, must be modelled in order for the equation set to be solved. Additionally, coupling to a Lagrangian particle tracking routine requires further modelling in that instantaneous velocities must be reconstructed from the time-averaged values using another mathematical approach. In terms of the accuracy of these methods, DNS involves no assumptions regarding the flow field, with LES only requiring assumptions for the smallest scales of turbulent motion. In contrast, RANS methods embody a significant modelling component, and as such cannot be expected to be as accurate as simulation techniques. RANS is in general the preferred tool for use in industry, as available in commercial computational fluid dynamic codes, and has reasonable computer run times. LES and DNS require significantly more computational resources, with DNS being restricted in terms of the Reynolds number and flow complexity it can handle as a consequence.

In the present work, RANS and LES methods are used to simulate the Eulerian flow field, and a Lagrangian approach is applied for particle tracking, with particle dispersion, deposition and re-suspension in a straight square duct explored. In terms of the comments above, LES results can be considered to more reliable and accurate than those from RANS due to the increased accuracy of the turbulent flow information that it generates.

Modelling and Simulation Methodologies

RANS model predictions were based on steady state solutions of the transport equations, expressing conservation of mass and momentum, for an incompressible Newtonian fluid with constant properties. These equations were written in appropriate forms for solution, with the unknown Reynolds stresses approximated through the use of a turbulence model. In this work, the Reynolds stresses were obtained directly from solutions of modelled partial differential transport equations, with the redistributive fluctuating pressure term as given in [22]. Wall reflection effects were also incorporated into this closure. This term represents a correction to the standard redistributive fluctuating pressure term, included to allow for the influence of pressure reflections from the surface in distorting the fluctuating pressure field away from the wall. In this work, the term was taken from [23]. Being linear in the Reynolds stress, this expression is consistent with the uniqueness arguments invoked by Jones and Musonge [22] in constructing the linear form used in the turbulence model. The expression is redistributive, and involves terms associated with the mean rate of strain, which have been found [24] to be of greater significance than those involving fluctuating velocities alone. Brasseur and Lee [24] also demonstrated that the "return" part of the pressure-rate of strain term is associated with much finer scale motions than the "rapid" component, such that the latter component might be expected to be more affected by the presence of any solid surface. The model was completed through solution of the turbulence energy dissipation rate equation, with all model constants taken as standard.

In large eddy simulation only the large energetic scales of motion are directly computed, whilst the small scales are modelled. Any function is decomposed using a localised filter function, such that filtered values only retain the variability of the original function over length scales comparable to or larger than that of the filter width. The present work used a top-hat filter as this fits naturally into a finite-volume formulation. This decomposition is then applied to the Navier-Stokes equations, for an incompressible Newtonian fluid with constant properties, giving rise to terms which represents the effect of the sub-grid scale (SGS) motion on the resolved motion. The SGS stress model used was the dynamic model of Germano et al. [25], implemented using the approximate localization procedure of Piomelli and Liu [26] together with the modification proposed by di Mare and Jones [27]. This model represents the SGS stress as the product of a SGS viscosity and the resolved part of the strain tensor, and is based on the possibility of allowing different values of the Smagorinsky constant at different filter levels. Test-filtering was performed in all space directions, with no averaging of the computed model parameter field.

RANS and LES Computations were performed using the computer program BOFFIN [28]. The code implements an implicit finite-volume incompressible flow solver using a co-located variable storage arrangement. Because of this arrangement, fourth-order pressure smoothing, based on the method proposed by Rhie and Chow [29], is applied to prevent spurious oscillations in the pressure field. Time advancement is performed via an implicit Gear method for all transport terms, and the overall procedure is second-order accurate in both space and time. The time step is chosen by requiring that the maximum Courant number lies between 0.1 and 0.3 for reasons of accuracy.

From the instantaneous fluid velocity field, particle motion was modelled using a Lagrangian particle tracking approach [30] in which the particles are followed along their trajectories through the unsteady, non-uniform flow field. To simplify the analysis, the following assumptions were made: the particle-laden flow is dilute; interactions between particles are negligible; the flow and particles are one-way coupled, i.e. the effect of particles on the fluid is neglected; all particles are rigid spheres with the same diameter and density; and particle-wall collisions are elastic. The particle trajectory, which is governed by Newton's second law, was then determined by solution of the particle equation of motion which involves terms for the forces on a particle. Even though a number of possible forces can act on a particle, many of these may be neglected without any appreciable loss of accuracy, depending on the particle inertia. The most important force acting on a particle is the Stokes drag force, with gravity also important depending on the orientation of the flow. In this study, Stokes drag, gravity and buoyancy forces were considered in terms of particle deposition, although the shear-induced Saffman lift force [31] was neglected because it only assumes non-trivial magnitudes in the viscous sub-layer. Even in this region, however, it has been found to be an order of magnitude smaller than the normal component of the Stokes drag force [32]. The lift force was, however, incorporated in predicting particle re-suspension effects. Other forces acting on the particle were not taken into account due to their being orders of magnitude smaller than the effects considered [33]. The fluid velocities required in the above method are instantaneous, and therefore a technique is needed to derive such velocities from the time-averaged information supplied by the RANS approach. In this work a random Fourier series method [30] was used to generate these velocities, with instantaneous velocities derived from time-averaged and fluctuating values.

A fourth-order Runge-Kutta scheme was used to solve the equation of motion, given the initial particle location and velocity. Initial particle positions were distributed randomly throughout the duct, corresponding to an initially uniform wall-normal particle number density profile. Initial particle velocities were set equal to the fluid velocity. Particles were assumed to interact with turbulent eddies over a certain period of time, that being the lesser of the eddy lifetime and the transition time. For particles that moved out of the square duct in the streamwise direction for the straight duct flows, periodic boundary conditions were used to reintroduce them into the computational domain.

Results and Discussion

Particle deposition in turbulent duct flows was considered using LES and RANS. The flow considered was three-dimensional and described using a Cartesian co-ordinate system (*x, y, z*) in which the *z* axis was aligned with the streamwise direction, the *x* axis was in the direction normal to the floor of the duct, and the *y* axis was in the spanwise direction. The corresponding velocity components in the (*x, y, z*) directions are (*u, v, w*), respectively. The flow Reynolds number was 250,000 based on the flow bulk velocity. Importantly, in ducts secondary flows are established in the duct cross-section that transfer streamwise momentum from the centre of the duct towards the corner regions. The mean secondary flows display a high degree of symmetry about the corner bisector, with two counter-rotating vortices in each corner of the duct, and four pairs of vortices in the duct as a whole.

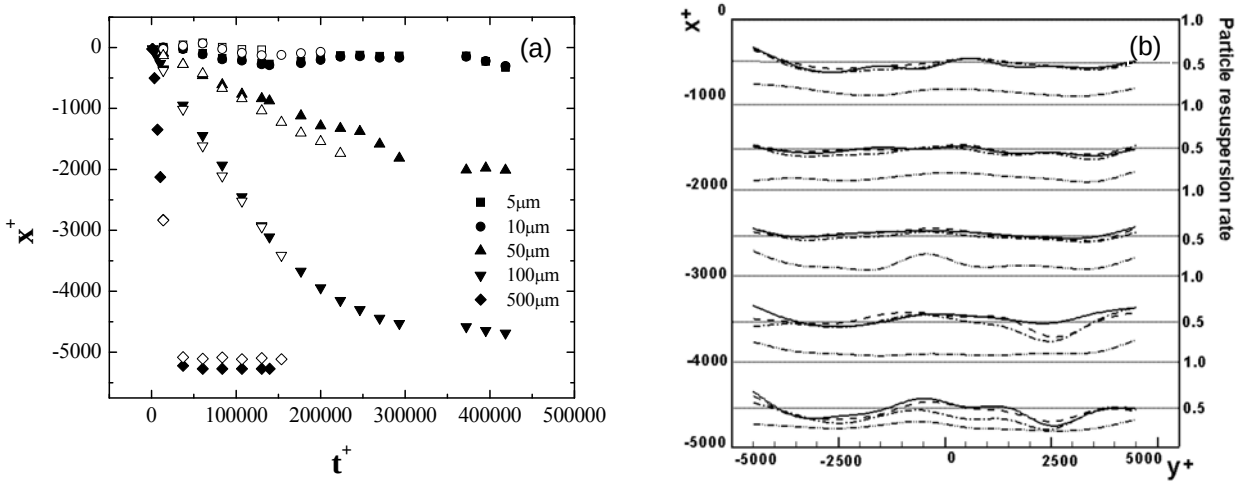

Fig. 4. (a) Particle dispersion with time in the vertical direction in terms of the particle mean displacement (open symbols LES, closed symbols RANS), and (b) particle re-suspension rate for different sizes of particle (—· 5, --- 50, -·- 100 and -···- 500 μm particles).

Fig. 4(a) shows results for the time-dependent particle dispersion in the vertical direction, where x^+ is the vertical distance and t^+ the time, both in wall units. In this figure the mean value of the particle displacement is seen to generally decrease with time due to gravity effects, with the rate of deposition increasing with particle size. For the 500 μm particles it only takes a short time for them to approach the duct floor, whilst for medium sized particles (50 and 100 μm) the rate of deposition is slower and linear with time, with that rate increasing with particle size. For small particles (5 and 10 μm), the mean value of the particle displacement in the vertical direction generally stays constant, although slightly oscillatory. Overall, there is excellent agreement between the LES and RANS predictions, although there is a slight under-prediction of the rate of deposition of the 50 μm particles by the RANS. These results were also analysed in terms of the particle dispersion function which gives an indication of the location of the particles relative to their mean position. It was clear from these results that for particles of 100 μm and larger the function decreases relatively rapidly with time, whilst for particles up to 50 μm in diameter the dispersion function remains approximately constant. Closer examination of the LES results for the latter particles did, however, indicate that whilst the 5 and 10 μm particles disperse more in the vertical direction, dispersion for the 50 μm particles increases with time until $t^+ \approx 100{,}000$, after which point it starts to decrease due to deposition. In general, RANS results were in line with the LES predictions, although for the 5, 10 and 50 μm particles the dispersion function was seen to vary more with time, although remaining approximately constant on average.

Equivalent results in the spanwise direction showed that mean values of the particle displacement vary with time for all particle sizes, although for the LES the variation increased with size indicating that small particles tend to disperse well in this direction. For particles of 50 μm and larger, the mean value of particle displacement in the vertical direction varied widely when compared to that in the spanwise direction. This suggests that for these particles the effect of gravity is more significant than that of the secondary flow. However, for small particles (5 and 10 μm), the dispersion in both directions was approximately the same, indicating that gravity effects are unimportant for such particles. RANS results were again generally in line with the LES, although there was more variability in these predictions, and significant differences for the 500 μm particles. This was further emphasized by results for the dispersion function in the spanwise direction. In particular, the LES predictions demonstrated that the largest particles deposit towards the floor of the duct with a significant spanwise motion, whereas the RANS predictions show that these particles deposit with little lateral movement. The consequence of this is that whilst in the LES the largest particles concentrate at the corners of the duct floor due to the influence of secondary flows within the duct, in RANS they deposit with a more even distribution. Analysis of the various forces acting on the particles, and mean relative slip velocities between the fluid and particles, indicated that the spanwise drag force acting on the largest particles was under-predicted by RANS, with the corresponding slip velocity similarly under-predicted.

Overall, these results demonstrate than the simpler RANS modelling technique is capable of predicting particle deposition in practically relevant flows. Duct flows are encountered in practice and, due to the secondary flows which arise in the cross-section of the duct, are also representative of the complexities found in other situations, such as pipe bends. Interestingly, the way in which the particles deposit is seen to differ between the LES and RANS, and this might lead to differences in whether or not pipe blockage would be predicted with any degree of accuracy. In the absence of any experimental data on such flows, the LES results provide a means by which the RANS formulation can be modified to improve its accuracy.

Particle re-suspension in turbulent duct flows has also been investigated using LES for the same geometry and flow conditions considered above. Particle re-suspension is considered here in terms of multiple particles moving away from locations close to the floor of the duct, i.e. simulating the re-suspension of particles from a solid bed formed on the duct floor. Re-suspension is therefore considered in the x direction in what follows. Four sizes of particle, 5, 50, 100 and 500 μm were considered in these computations in order to allow a statistical analysis of the results. Fig. 4(b) shows results for the rate of particle re-suspension obtained at $t^+ = 9{,}303$. In this figure, the lower half of the duct is separated equally into five regions in the x direction, with the re-suspension rate profiled in each. In order to investigate the influence of secondary flow effects on particle behaviour, the lift force is not considered in the results of this figure. For all sizes of particle, re-suspension is seen to be dominant in two regions: one close to the central plane ($y^+ = 0$) of the duct, and the other close to the side-walls ($y^+ = \pm 5274$). This observation is in line with these regions coinciding with locations where secondary flow within the duct provides a strong upward motion. Apart from in these two regions, particle-deposition appears to dominate elsewhere in the duct. From the results of Fig. 4(b), particle re-suspension is seen to decrease with height in the duct, which is as might be anticipated given the need for particles to overcome the effects of gravity in order to re-suspend within the flow. Additionally, the strength of the secondary flows decreases with height [34]. It may also be noted that smaller particles tend to re-suspend in preference to larger ones, again as might be anticipated given the smaller influence of gravity on these particles, and the fact that they respond more rapidly to the flow due to their lower aerodynamic response time. This is in contrast to large particles whose response time is greater than the characteristic time scale of the large-scale vortex structures in the flow. As a result, such particles respond very slowly to changes in the flow field. It is worth noting that in this figure less than 50% of the largest (500 μm) particles re-suspend in all the regions considered, suggesting that for such particles deposition within the flow is dominant. Furthermore, for these particles re-suspension appears to be greatest close to the floor of the duct where particle-wall collisions are influential. From this analysis it may be concluded that the secondary flow dominates the particle re-suspension process considered.

Overall, this study demonstrates that particle re-suspension occurs provided that the drag force on a particle overcomes the gravity effect, which is significantly determined by the secondary flows since re-suspension occurs preferentially at locations where they are influential. The gravitational force is an important factor acting against particle re-suspension. The lift force acting on a particle has also been shown to increase greatly with particle size, with its influence increasing as a particle approaches the duct wall. For small particles, the drag force (secondary flow) dominates particle re-suspension, while for large particles the lift force also contributes. In the vertical direction, small particles are found to more readily re-suspend than large particles. This study has therefore provided

fundamental physical insights into the particle re-suspension process, and its results will be used in future to allow the formulation and validation of simpler RANS-based approaches for use in process design.

CONCLUSIONS

The link between the surface charge characteristics of particles and their resulting aggregation and rheological properties can be used to aid in the prediction of slurry behaviour. Results presented suggest that by assessing the solution pH and conductivity conditions in legacy waste ponds, one may be able to qualitatively estimate dispersion yield stresses by using particle zeta potential data. These results highlight a general guiding rule linking particle-particle interactions to bulk slurry behaviour, this being that dispersion yield stresses are greatly enhanced in conditions close to the isoelectric point. Further, AFM data demonstrates that regardless of solution pH, the effects of solution salt lead to attractive particle-particle interactions and hence coagulation in oxide systems.

Studies of particle flows in pipes have established the minimum transport velocity, with a lower velocity measured for an aggregated than for a dispersed suspension. This finding is believed to relate to differences in turbulence levels within the flow, and of practical relevance since it shows that the energy input to maintain particles in suspension can be lowered if aggregates are present. It has also been demonstrated that the intensity of turbulence can be affected by solid particles, with small particles attenuating turbulence levels and large particles augmenting them. The coagulation of particles is also of importance, with turbulence levels augmented by agglomerates at low Reynolds numbers, but with high turbulence levels destroying them and reducing their effect on the carrier fluid.

Two different computational fluid dynamic techniques have been applied to simulate particle-laden flows in a straight square duct, with Eulerian flow solutions coupled to a Lagrangian particle tracking routine to predict particle trajectories. It has been demonstrated that the mean value of the particle displacement in a straight square duct flow generally decreases with time due to gravity effects, with the rate of deposition increasing with particle size. Particle re-suspension has been studied in a duct flow and the process shown to be dominated by the secondary flows, with smaller particles tending to re-suspend in preference to larger ones.

The potentially significant economic and health costs involved with improper processing of nuclear legacy wastes means that traditional trial-and-error process design is not appropriate. Hence, being able to accurately predict slurry activity, say during re-dispersion and pumping, is of utmost importance. All the work described in this paper has shown that by the correct analysis of complementary and relatively inexpensive laboratory based techniques, and the application of mathematical models, a high level of system detail can be gathered which is of benefit in enhancing our understanding of these slurries, which in turn is of value in enabling the design of cost effective and efficient nuclear waste treatment processes.

ACKNOWLEDGEMENTS

Much of the work described in this paper was carried out as part of the TSEC programme KNOO and as such we are grateful to the EPSRC for funding under grant EP/C549465/1. The financial support of the Nuclear Decommissioning Authority and the National Nuclear Laboratory is also gratefully acknowledged.

REFERENCES

1. R.W. O'BRIEN, "Electroacoustic Effects in a Dilute Suspension of Spherical Particles", J. Fluid Mech., 190, 71-86 (1988).
2. R.W. O'BRIEN, "The Electroacoustic Equations for a Colloidal Suspension", J. Fluid Mech., 212, 81-93 (1990).
3. R.W. O'BRIEN, D.W. CANNON, and W.N. ROWLANDS, "Electroacoustic Determination of Particle Size and Zeta Potential", J. Colloid Interface Sci., 173, 406-418 (1995).
4. J.S. DUNCAN, "Colloid and Surface Chemistry", 4th Edition, Butterworth Heinemann, Elsevier Science Ltd., Oxford (1992).
5. Q.D. NGUYEN, and D.V. BOGER, "Transporting Highly Concentrated Bauxite Residue to Disposal", J. Rheol., 27, 321-349 (1983).
6. G.V. FRANKS, S.B. JOHNSON, P.J. SCALES, D.V. BOGER, and T.W. HEALY, "Ion-Specific Strength of Attractive Particle Networks", Langmuir, 15, 4411-4420 (1999).

7. B.V. DERJAGUIN, and L. LANDAU, "Theory of the Stability of Strongly Charged Lyophobic Sols and of the Adhesion of Strongly Charged Particles in Solutions of Electrolytes", Acta Physicochim., URSS, 14, 633-662 (1941).
8. T.F. TADROS, "Solid/Liquid Dispersions", Academic Press, London (1987).
9. C. BINNIE, M. KIMBER, and G. SMETHURST, "Basic Water Treatment", Third Edition, Royal Society of Chemistry, Thomas Telford Ltd., Cambridge (2002).
10. R.A. GORE, and C.T. CROWE, "Effect of Particle Size on Modulating Turbulent Intensity", Int. J. Multiphase Flow, 15, 279-85 (1989).
11. G.V. FRANKS, Y. ZHOU, Y. YAN, G.J. JAMESON, and S.R. BIGGS, "Effect of Aggregate Size on Sediment Bed Rheological Properties", Phys. Chem. Chem. Phys., 6, 4490-4498 (2004).
12. E.J.W. VERWEY, and J.T.G. OVERBEEK, "Theory of the Stability of Lyophobic Colloids", Elsevier, Amsterdam (1948).
13. S. KIM, K.B. LEE, and C.G. LEE, "Theoretical Approach on the Turbulence Intensity of the Carrier Fluid in Dilute Two-Phase Flows", Int. Commun. Heat Mass, 32, 435-444 (2005).
14. R. ZISSELMAR, and O. MOLERUS, "Investigation of Solid-Liquid Pipe Flow with Regard to Turbulence Modification", Chem. Eng. J., 18, 233-239 (1979).
15. Z. YANG, X.F. PENG, and D.J. LEE, "Advective Flow in Spherical Floc", J. Colloid Interface Sci., 308, 451-459 (2007).
16. I.J. WYGNANSKI, and F.H. CHAMPAGNE, "On Transition in a Pipe. Part 1. The Origin of Puffs and Slugs and the Flow in a Turbulent Slug", J. Fluid Mech., 59, 281-335 (1973).
17. Y. TSUJI, "Activities in Discrete Particle Simulation in Japan", Powder Technol., 113, 278-286 (2000).
18. C. CROWE, R. TROUTT, and J. CHUNG, "Numerical Models for Two-Phase Turbulent Flows", Annu. Rev. Fluid Mech., 28, 11-43 (1996).
19. B. VAN WACHEM, and A. ALMSTEDT, "Methods for Multiphase Computational Fluid Dynamics", Chem. Eng. J., 96, 81-89 (2003).
20. F. MASHAYEK, and R. PANDYA, "Analytical Description of Particle/Droplet-Laden Turbulent Flows", Prog. Energy Combust. Sci., 29, 329-378 (2003).
21. J.S. CURTIS, and B. VAN WACHEM, "Modeling Particle-Laden Flows: A Research Outlook", AIChE J., 50, 2638-2645 (2004).
22. W.P. JONES, and P. MUSONGE, "Closure of the Reynolds Stress and Scalar Flux Equations", Phys. Fluids, 31, 3589-3604 (1988).
23. M. DIANAT, M. FAIRWEATHER, and W.P. JONES, "Reynolds Stress Closure Applied to Axisymmetric Impinging Turbulent Jets", Theor. Comput. Fluid Dynam., 8, 435-447 (1996).
24. J.G. BRASSEUR, and M.J. LEE, "Local Structure of Intercomponent Energy Transfer in Homogeneous Turbulent Shear Flow", Stanford University, Center for Turbulence Research, Proceedings of the Summer Program (1987).
25. M. GERMANO, "A Proposal for Redefinition of the Turbulent Stresses in the Filtered Navier-Stokes Equations", Phys. Fluids, 19, 2323-2324 (1986).
26. U. PIOMELLI, and L. LIU, "Large Eddy Simulation of Rotating Channel Flows Using a Localized Dynamic Model", Phys. Fluids, 7, 839-848 (1995).
27. L. DI MARE, and W.P. JONES, "LES of Turbulent Flow Past a Swept Fence", Int. J. Heat Fluid Flow, 24, 606-615 (2003).
28. W.P. JONES, "BOFFIN: A Computer Program for Flow and Combustion in Complex Geometries", Dept. Mech. Eng., Imperial College of Science, Technology and Medicine (1991).
29. C.M. RHIE, and W.L. Chow, "Numerical Study of the Turbulence Flow Past an Airfoil with Trailing Edge Separation", AIAA J., 21, 525-1532 (1983).
30. J.R. FAN, J. YAO, and K.F. CEN, "Antierosion in a 90° Bend by Particle Impaction", AIChE J., 48, 401-1412 (2002).
31. P.G. SAFFMAN, "Lift on a Small Sphere in a Slow Shear Flow", J. Fluid Mech., 22, 385-400 (1965).
32. J.B. MCLAUGHLIN, "Aerosol Particle Deposition in Numerically Simulated Channel Flow", Phys. Fluids, 1, 1211-1224 (1989).
33. V. ARMENIO, and V. FIOROTTO, "The Importance of the Forces Acting on Particles in Turbulent Flows", Phys. Fluids, 13, 2437-2440 (2001).
34. M. FAIRWEATHER, and J. YAO, "Mechanisms of Particle Dispersion in a Turbulent, Square Duct Flow", AIChE J., 55, 1667-1679 (2009).